Crystallins Play a Crucial Role in Glaucoma and Promote Neuronal Cell Survival in an In Vitro Model Through Modulating Müller Cell Secretion

Hanhan Liu,[1] Katharina Bell,[2] Anja Herrmann,[3] Stefan Arnhold,[3] Karl Mercieca,[4] Fabian Anders,[5] Kerstin Nagel-Wolfrum,[6] Solon Thanos,[7] and Verena Prokosch[1]

[1]Department of Ophthalmology, Faculty of Medicine and University Hospital of Cologne, University of Cologne, Cologne, Germany
[2]Singapore Eye Research Institute and Singapore National Eye Center, Singapore; Duke-NUS Medical School, Singapore
[3]Institute of Veterinary Anatomy, Histology and Embryology, Justus-Liebig-University Gießen, Gießen, Germany
[4]Department of Ophthalmology, University Medical Center Bonn, Bonn, Germany
[5]Department of Ophthalmology, University Medical Centre of the Johannes Gutenberg University Mainz, Mainz, Germany
[6]Institute for Molecular Physiology, Johannes Gutenberg University Mainz, Mainz, Germany
[7]Department of Ophthalmology, Experimental Ophthalmology, University Medical Center Münster, Münster, Germany

Correspondence: Hanhan Liu, Department of Ophthalmology, Faculty of Medicine and University Hospital of Cologne, University of Cologne, Kerpner Str. 62, 50937 Cologne, Germany; hanhan.liu@uk-koeln.de.

Received: January 21, 2022
Accepted: May 13, 2022
Published: July 11, 2022

Citation: Liu H, Bell K, Herrmann A, et al. Crystallins play a crucial role in glaucoma and promote neuronal cell survival in an in vitro model through modulating Müller cell secretion. *Invest Ophthalmol Vis Sci.* 2022;63(8):3. https://doi.org/10.1167/iovs.63.8.3

Purpose. The aim of this study was to explore the roles of crystallins in the context of aging in glaucoma and potential mechanisms of neuroprotection in an experimental animal model of glaucoma.

Methods. Intraocular pressure (IOP) was significantly elevated for 8 weeks in animals at different ages (10 days, 12 weeks, and 44 weeks) by episcleral vein cauterization. Retinal ganglion cells (RGCs) were quantified by anti-Brn3a immunohistochemical staining (IHC). Proteomics using ESI-LTQ Orbitrap XL-MS was used to analyze the presence and abundance of crystallin isoforms the retinal samples, respectively. Neuroprotective property and localization of three selected crystallins *CRYAB*, *CRYBB2*, and *CRYGB* as most significantly changed in retina and retinal layers were determined by IHC. Their expressions and endocytic uptakes into Müller cells were analyzed by IHC and Western blotting. Müller cell secretion of neurotrophic factors into the supernatant following *CRYAB*, *CRYBB2*, and *CRYGB* supplementation in vitro was measured via microarray.

Results. IOP elevation resulted in significant RGC loss in all age groups ($P < 0.001$). The loss increased with aging. Proteomics analysis revealed in parallel a significant decrease of crystallin abundance – especially *CRYAB*, *CRYBB2*, and *CRYGB*. Significant neuroprotective effects of *CRYAB*, *CRYBB2*, and *CRYGB* after addition to retinal cultures were demonstrated ($P < 0.001$). Endocytic uptake of *CRYAB*, *CRYBB2*, and *CRYGB* was seen in Müller cells with subsequent increased secretion of various neurotrophic factors into the supernatant, including nerve growth factor, clusterin, and matrix metallopeptidase 9.

Conclusions. An age-dependent decrease in *CRYAB*, *CRYBB2*, and *CRYGB* abundance is found going along with increased RGC loss. Addition of *CRYAB*, *CRYBB2*, and *CRYGB* to culture protected RGCs in vitro. *CRYAB*, *CRYBB2*, and *CRYGB* were uptaken into Müller cells. Secretion of neurotrophic factors was increased as a potential mode of action.

Keywords: experimental glaucoma, crystallins, cell culture, neuroprotection, neurotrophic factors, Müller cells

Glaucoma is one leading cause of irreversible blindness worldwide, characterized by progressive loss of retinal ganglion cells (RGCs) and damage to the optic nerve head.[1] Elevated intraocular pressure (IOP) is the major risk factor of glaucoma and also the only risk factor that can be targeted and treated in current clinical practice.[2] However, as the underlying pathogenesis of glaucoma remains elusive, controlling IOP is not enough to halt the progress of the loss of visual function in a significant proportion of patients.[3] Besides elevated IOP, aging is an important risk factor with the incidence of glaucoma increasing significantly in the aged population.[4] Molecular processes leading to this age-related RGC susceptibility to neurodegeneration are largely unknown.

Crystallins might play a pivotal role in this context.[5–8] Crystallins, comprised of the alpha-, beta-, and gamma-subclasses in all vertebrate classes,[9–11] are the predominant structural proteins in the lens, evolutionarily related to stress proteins. More recently, crystallins were found to be abundant in the retina.[11] They are associated with neurodegenerative diseases within the retina, such as ischemia–reperfusion injury, glaucoma, and diabetic retinopathy.[12–16]

Besides that, mutations of crystallins are related to age and neurodegenerative diseases, including Parkinson's disease, Alzheimer's disease, multiple sclerosis, and Huntington's disease.[17–19]

We have shown that expression of the crystallin proteins within the retina is upregulated in response to elevated IOP. Furthermore, we could show that this reaction is age dependent. Alpha-crystallins show a high homology with small heat shock proteins (HSPs) and tend to function as distinct anti-apoptotic regulators, with a chaperone-like activity upon external stimuli. Alpha-B crystalline has been shown to be neuroprotective.[20–23] Beta- and gamma-crystallins form their own superfamily and have shown neuroprotective and neuroregenerative properties on retinal neurons both in vitro and in vivo, whereas the underlying mechanism cells and interaction partners remain unclear.[24–26]

Increased levels of α-crystallins have been found in glial cells in several models of neuroinflammation[13,27,28] in association with activation of astrocytes. It is assumed that α-crystallins regulate astrogliosis in response to inflammatory signals.[29,30] Interestingly, crystallins of the β/γ superfamily are reported to upregulate the expression of both *CNTF* and STAT3 in the retina, in cultures, and in vivo.[31,32] However, the exact mechanisms are still unknown.

Müller glial cells (MGCs) have a fundamental role for the maintenance of retinal homeostasis and their interaction with most other retinal cells is well documented.[33] Müller cells are not only essential for structural reasons but also for the role they have in the complex molecular network of activation/response of the sensory neuroretina under stressful conditions as it occurs in traumas or diseases characterized by the cascade of inflammation.[34] In response to injury or disease, Müller cell's stress reaction is primarily thought to be protective through secretion of growth factors and regulation of other pro-survival effects.[30] Via secretion, retinal Müller cells act as an endogenous source of neurotrophic factors, such as ciliary neurotrophic factor (*CNTF*) or brain-derived neurotrophic factor (*BDNF*).[35,36] Although there is a link that crystallins affect gliosis and play a role in several models of neuroinflammation including glaucoma, there exact role of action has not been described.

Therefore, we aimed to analyze the age-dependent expression of specific crystallins, unravel the neuroprotective potential of the crystallins in more detail by understanding their distribution in Müller cells, and their potential mode of action.

Methods

Animal Treatment and Ethical Statement

All experiments were conducted in accordance with the Association of Research in Vision and Ophthalmology (ARVO) Statement for the Use of Animals in Ophthalmic and Vision Research. The study was approved by the ethics committee of animal research Rhineland-Palatinate (permission number: 14-1-085). Exclusively female Sprague Dawley rats (n = 22) were used in this study. All animals were housed in the Translational Animal Research Center (TARC) of the Johannes-Gutenberg University Mainz. The animals are kept in groups and provided with litter, nesting material, and nest boxes under a regular 12-hour day-night cycle. Food and water were provided ad libitum. The animals are examined daily for changes of the eye and abnormal behavior by trained staff members of the TARC. During all interventions, minimizing pain and indisposition for the animals was at highest priority. In total, 26 rats were included in this study. Different aged animals aged 10 days, 12 weeks, and 44 weeks at the time of the first intervention were used (10 days: $n = 7$, 12 weeks: $n = 7$, and 44 weeks: $n = 7$). Another 5 animals at the age of 8-weeks were used for in vitro retinal culture.

Experimental Glaucoma Induction and Intraocular Pressure Determination

The experimental glaucoma model was carried out through episcleral vein occlusion (EVO) of only the left eyes to create a constant IOP elevation for period of 7 weeks, the right eyes of the animals were left untouched and used as control. The EVO technique in rats was first described by Shareef et al. in 1995.[37] In brief, the animals were under general anesthesia, with intraperitoneal Ketamin (Ketamin Inresa, 100 mg/kg; Inresa Arzneimittel GmbH, Germany) plus medetomidine hydrochloride (Xylazin, 10 mg/kg; Dorbene, Zoetis, Germany) injection. Oxybuprocaine eye drops (Novesine, OmniVision, Germany) were applied topically onto the ocular surface. The conjunctiva and tenon was opened carefully and three of the five episcleral vein-trunks were cauterized using a medical cauterization device (Bovie Medical Corporation, USA). After the surgery, novaminsulfon (Novalgin, Ratiopharm, Ulm, Germany) was added to water tanks to minimize postoperative pain for the following 3 days. The IOP was measured right before performing EVO and on a weekly basis postoperatively using a Tonolab device (iCare, Finland). The animals were awake and not anesthetized during the IOP measurements. Topical anesthesia was applied (Novesine, OmniVision, Germany) and only slightly fixated through handholding. Ten IOP readings were taken per measurement and subsequently averaged. Animals with fluctuating IOPs or no signs of IOP elevation were excluded from the study (10 days: n = 2, and 44 weeks: $n = 2$).

Preparation of Retinal Explants

Five Sprague-Dawley rats were euthanatized by CO_2. Eyes were enucleated immediately postmortem and transferred to a petri dish containing ice-cold betaisodona solution (Braunol, Braun, Germany) for 3 minutes. The eyes were then dissected in ice cold sterile Hank's Balanced Salt Solution (HBSS; Gibco BRL, Eggenstein, Germany). The anterior segment of the eye was detached, and the intact retina was separated from the optic cup and flat mounted on Millipore filters (Millipore; Millicell, Cork, Ireland), with the ganglion cell layer facing upward. Vitreous body was removed carefully subsequently.

Retinal Sample Preparation for Liquid-Chromatography Electrospray Ionization Mass Spectrometry

For protein extraction, retinal tissue was shock frozen with liquid nitrogen and disintegrated to powder in a mortar. The samples were incubated in lysis buffer (0.5% n-dodecyl-β-D-maltoside in 20 mM Tris-buffered saline) at 4°C for 1 hour and another hour in ultrasonic bath on ice to ensure a maximum of cellular breakdown. Protein concentration of each sample was determined by standard bicinchoninic acid

Investigative Ophthalmology & Visual Science

(BCA) protein assay kit (Pierce, Rockford, IL, USA) following the instruction of the manufacturer. From each retinal elute, 80 µg of protein was loaded onto a NuPAGE Novex 12% Bis-Tris Protein Gel (Thermo Fisher, USA) and was subjected to polyacrylamide gel electrophoresis (PAGE). Each gel lane was divided into 15 individual pieces and de-stained using ammonium bicarbonate (Sigma Aldrich, USA) and acetonitrile (AppliChem, Germany), reduced, alkylated, dehydrated, and digested with sequence grade trypsin (Promega, USA) at 37°C overnight.[38] The extracted peptides were further purified by C-18 ZipTips (Merck, Germany) as per the manufacturer's protocol.[39] The samples were then dehydrated and stored at −20°C until further mass spectrometry (MS) measurement.

MS Measurement

The MS measurement was conducted as previously published.[5] The continuum MS data were collected by an ESI-LTQ Orbitrap XL-MS system (Thermo Scientific, Bremen, Germany) and searched against UniProt database with MaxQuant software version 1.5.3.30 (Max Planck Gesellschaft, Germany).[40] A target-decoy-based false discovery rate (FDR) was set to 0.01 for identification of peptides and proteins, the minimum peptide length was 6 amino acids and the minimum unique peptides were set at 2. Fold-changes of the label-free quantitation (LFQ) intensities were calculated to identify the significantly differentially expressed proteins (Supplementary Data S1).

Cultivation of Retinal Explants With Crystallins

To study the neuroprotective effects of the crystallins, retinal explants of untreated rats ($n = 5$) were cut equally into 4 pieces and each piece was transferred into culture medium in a Lumox dish 35 (Sarstedt, Nümbrecht, Germany). The culture medium contains Dulbecco's Modified Eagle's Medium/Nutrient Mixture F-12 (DMEM/F12; Gibco BRL, Eggenstein, Germany), supplemented with 15 mM HEPES (Sigma Aldrich, Germany), 100 U/mL penicillin, 100 µg/mL streptomycin medium with or without the addition of 200 µg/L crystallins, α-crystallin B (*CRYAB*), β-crystallin B2 (*CRYBB2*), and γ-crystallin B (*CRYGB*; Polyclonal Antibody, Biossua). The Lumox dishes were then placed into a high-pressure incubation chamber and incubated pressurized by 60 mm Hg for 48 hours. The retinal tissue was cultured i, and aerated with humidified 5% CO_2, balance air, at 37°C. The home-made pressure chamber allows accurate increase of hydrostatic pressure at 37°C, with sufficient turnover of 5% CO_2 and air, more details can be found in our previous study.[41] The retinas explanted from the adult Sprague Dawley rat were cultivated in flat mount under different conditions. Retinal explants without cultivation served as a control. As further control groups, explants were cultivated for 48 hours with or without 60 mm Hg hydrostatic pressure. Furthermore, explants were cultivated with additional *CRYAB*, *CRYBB2*, and *CRYGB* for 48 hours under 60 mm Hg pressure.

Quantification of RGCs

RGCs in retinal explants were labeled by the brain-specific homeobox/POU domain protein 3A (Brn3a, C-20 goat polyclonal IgG; Santa Cruz Biotechnology, USA) immunohistochemical staining.[42,43] Briefly the retinal explants were washed in phosphate-buffered saline (PBS), fixed in 4% paraformaldehyde (PFA; pH = 7.4; Carl Roth), and then in 30% sucrose solution for 12 hours, subsequently snap-frozen in methyl butanal (Merck, Germany). The explants were stained as previously described.[7] Immunofluorescent RGCs were visualized with a fluorescent microscope (Axiophot Carl Zeiss, Germany). Six pictures of different regions in the quarter of the retina were taken (20-fold magnification). Total numbers of the RGCs were countered using an ImageJ-macro (ImageJ Fiji version 1.51, total = 6 counts/quadrant, and 6 retinal quadrants per group), an average value was calculated and then extrapolated to RGCs/mm^2, the mean values were compared between groups. Primary antibodies used were Brn3a (C-20; 1:125; Santa Cruz Biotechnology; sc-31984). Secondary antibodies used were donkey anti-goat conjugated with Alexa Flour 558 (1:500; Life Technologies, A11507).

Immunodetection of Crystallins in Human and Rat Retina

Immunohistochemistry staining against α-crystallin B (*CRYAB*), β-crystallin B2 (*CRYBB2*), and γ-crystallin B (*CRYGB*) on frozen sections of retina from human donor eyes and Sprague-Dawley rats was performed. Human donor eyes ($n = 1$) were obtained through the University eye clinic eye bank after full consent by family members and in accordance with the Declaration of Helsinki. Briefly, sections were incubated with PBS containing 5% goat or donkey serum for 30 minutes, prior to overnight incubation with primary antibody at 4°C. Following the incubation, sections were washed in PBS, incubated with secondary antibody for 1 hour at room temperature, washed, drained, and mounted using DAKO Paramount (DAKO Corporation, Carpinteria, CA, USA). Primary antibodies used were *CRYAB* (1:200; Enzo Life Sciences, ADI-SPA-223); *CRYBB2* (1:200; Cloud Clone; PAF346Mu01); *CRYGB* (1:200; Abgent, San Diego, CA, USA, AP16201c). Secondary antibodies used were goat Anti-Rabbit IgG H&L (1:1000; Alexa Fluor 488). Immunohistochemical staining in paraffin sections of rat retina is performed using VECTASTAIN ABC AP Kits (AP, Vector Laboratories, Burlingame, CA, USA) following the manufacturer's introduction.

Isolation and Culture of Müller Cells From Porcine Eyes

The ocular bulbs of pigmented pigs (3–6 months, Piétrain breed) were obtained from a local slaughter house within 1 to 2 hours after slaughtering and kept in PBS on ice. The retinae were harvested under sterile conditions, no later than 3 hours after slaughtering. The method was described in detail in a previously published study.[44] The rationale for using pig eyes for this study was multifold. The pig eye not only has a similar size to the human eye, it also has a visual streak that is comparable to the human macula. In addition, it was important for us to use Müller cells derived from adolescent animals. The number of retinae needed to perform studies on Müller cells in vitro would have also meant using a substantial number of rats or mice to obtain these cells. We therefore decided to reduce animal usage with the additional benefits mentioned above and use adolescent pig retinae. Müller cells were isolated from dissociated retina with the Papain Dissociation Kit from Worthington (PDS LK003150l)

Investigative Ophthalmology & Visual Science

as per the manufacturer's protocol. The culture flasks were pretreated with 2 µg/cm^2 poly-D-lysin for 1 hour and with 1 µg/cm^2 laminin at 37°C for 2 hours in advance. The isolated cells were resuspended in DMEM/ Ham F-12 supplemented with 10% fcs, 100 U/mL penicillin, 100 U/mL streptomycin in three 75 cm^2 culture flasks. The first medium change took place 24 hours after isolation to remove nonadherent and foreign cells. Subsequently, the medium was replaced every 2 days. The cells were cultured for at least 7 days until they had completely differentiated and reached a confluence of over 90%, in order to be able to be passaged and used for further experiments. Immunohistochemistry staining against Müller cell marker, glutamine synthetase, and RGC marker, Brn3a, was performed to analyze the number of Müller cells in the percentage and RGCs in the culture. After 7 days in vitro (DIV), we obtained a pure Müller cell culture, which was positive for glutamine synthetase and negative for Brn3a and other retinal markers.

Detection of Endogenous Crystallins in Müller Cells

For the detection of endogenous crystallins present in Müller cells, the Müller cells were seeded in 48-well plates of 15,000 cells in each well, incubated overnight at 37°C in the incubator to allow adherence, and stained immunohistochemically the next day at a confluence of 70% to 80%. Briefly, the cells were washed 3 times with PBS, fixed with 4% PFA, permeabilized with 0.1% Triton X-100 (Sigma Aldrich) for 5 minutes and blocked with 1% bovine serum albumin (BSA; Sigma-Aldrich) and 0.05% TWEEN-20 (Sigma Aldrich) in PBS for 45 minutes at room temperature. The cells were incubated with primary antibodies against crystallins at 4°C overnight. Primary antibodies used were *CRYAB* (1:200; Enzo Life Sciences, ADI-SPA-223); *CRYBB2* (1:200; Cloud Clone; PAF346Mu01); and *CRYGB* (1:200; Abgent; AP16201c).

After washing with PBS, the Müller cells were further incubated with HRP-conjugated goat anti-rabbit secondary antibody at room temperature. Secondary antibodies used were goat anti-rabbit, conjugated with HRP (1:800; Sigma Aldrich; 12-348). The cell nuclei are labeled by DAPI (1:2500). Immunofluorescent Müller cells were visualized with a fluorescent microscope (Axiophot; Carl Zeiss, Germany).

Detection of Crystallin Uptake in Müller Cells

For the analysis of the crystallin uptake by fluorescence microscopy, 15,000 Müller cells were seeded per well in a 48-well plate. For subsequent Western blot analysis, 300,000 Müller cells/well were seeded in 6-well plates. The seeded cells were incubated overnight at 37°C to allow grow and re-adherence. The following day, the cells were incubated for 1 hour with culture medium as a control or with additional 6.67 µg/mL *CRYAB* (Abcam), *CRYBB2* (Cloud Clone), and *CRYGB* (CUSABIO), respectively.

Analyzing Crystallin Uptake Via Fluorescence Microscopy

Primary Müller cells were incubated for 1 hour with basic medium or with additional *CRYAB*, *CRYBB2*, or *CRYGB* labeled with Mix-n-Stain CF555 Antibody Labeling Kit (Sigma Aldrich, St. Louis, MO, USA). This dye bound covalently to the crystallins and their antibodies. After the incubation of the respective crystallin, the Müller cells were washed twice with PBS and fixed with cold 4% PFA. The cell nuclei were labeled by DAPI. The Müller cells and the labeled uptaken crystallins were visualized with a fluorescent microscope (Axiophot; Carl Zeiss, Germany). Images through the DAPI channel and the TRITC channel were obtained in the defined position from each well.

Analyzing Crystallin Uptake Via Western Blot

After 1 hour of incubation with basic medium or with additional *CRYAB*, *CRYBB2*, or *CRYGB*, the Müller cells were lysed as follows. The cells were washed twice with cold PBS and incubated in 70 µL lysis buffer, 4,4'-diaminodiphenylmethane (DDM; 1%+1% protease inhibitor), on ice. After 5 minutes of incubation, the cells were detached from the bottom of the well plate. The cell lysates were sonicated for 1 minute in an ultrasonic bath on ice and then centrifuged at 1500 g for 5 minutes, the supernatants were collected for further analysis.

Protein concentration of each lysate was determined by BCA Protein Assay Kit (Pierce, Rockford, IL, USA) as per the manufacturer's instructions. From each Müller cell lysate, 30 µg of protein was loaded onto a Novex NuPAGE 12% Bis- Tris polyacrylamide gel (Thermo Fisher, USA). The gel electrophoresis was ran using NuPAGE running buffer MES at 4°C with a voltage of 100 V and increased to 200 V after 10 minutes.

After electrophoresis, the proteins were blotted onto a nitrocellulose membrane using a wet transfer system (Bio-Rad, Hercules, CA, USA) and standard transfer buffer (with 20% methanol), a voltage of 20 V was applied for 15 minutes. Brief Ponceau red staining was performed to assess quality of the transfer as well as whole protein content. The signals of the crystallins were set in relation to the charge control and are presented in relative signal intensity.

Microarray Analysis of Müller Cells Secretome

Of the Müller cells, 45,000 were seeded into 24-well plates and allowed to grow and adhere to the surface overnight. The cells were pre-incubated with the proteins *CRYAB* (Abcam), *CRYBB2* (Cloud Clone), and *CRYGB* (CUSABIO) or control medium for 4 hours. Crystallins used in the cell culture medium were with a final concentration of 1.7 µg/mL ($n = 3$).

After incubation, the cells were washed twice with PBS and incubated with DMEM/Ham-F12 supplemented with reduced concentration of fetal calf serum (2%) for 16 hours. This medium is referred to as being the conditioned medium. Additional control medium was collected without conditioning through the cells ($n = 10$ for every experimental group).

Commercially available antibodies against different growth factors, comprising *BDNF*, *CNTF*, interleukin 6 (*IL-6*), transforming growth factor-beta 2 (*TGFb2*), transforming growth factor-beta 1 (*TGFb1*), pigment epithelium-derived factor (*PEDF*), apolipoprotein E (*ApoE*), nerve growth factor beta (*NGFb*), vascular endothelial growth factor A (*VEGFA*), clusterin (*CLU*), complement Factor H (*CFH*), and matrix metallopeptidase 9 (*MMP-9*; detailed information can be seen in Table 1) were used. These factors are known to be secreted by Müller cells and have an impact on the survival

Table 1. Antibodies Used in Microarray Analysis

Antibody	Distributer/Manufacturer
Rabbit anti-human *BDNF* antibody	Ab6201, Abcam, Cambridge, United Kingdom
Anti-ciliary neurotrophic factor (*CNTF*)	ABIN1585830, Antibodies Online GmbH, Aachen, Germany
Anti-interleukin 6 (*IL6*)	GTX79381, Enzo Life Sciences, Israel
Anti-transforming growth factor-beta 1 (*TGFb1*)	ABIN2998227, Antibodies Online GmbH, Aachen, Germany
Anti-transforming growth factor-beta 2 (*TGFb2*)	ABIN2992615, Antibodies Online GmbH, Aachen, Germany
Anti-pigment epithelium-derived factor (*PEDF*)	ABIN4237861, Antibodies Online GmbH, Aachen, Germany
Anti-apolipoprotein E (*ApoE*)	ABIN258785, Antibodies Online GmbH, Aachen, Germany
Anti-nerve growth factor beta (*NGFb*)	ORB11126, Biorybt, Cambridge, United Kingdom
Anti-vascular endothelial growth factor A (*VEGFA*)	Ab39250, Abcam, Cambridge, United Kingdom
Anti-clusterin (*CLU*)	ABIN1077938, Antibodies Online GmbH, Aachen, Germany
Anti-complement factor H (*CFH*)	PA5-24425, Thermo Fisher Scientific, Waltham, MA, United States
Anti-matrix metallopeptidase 9 (*MMP9*)	ABIN113587, Antibodies Online GmbH, Aachen, Germany

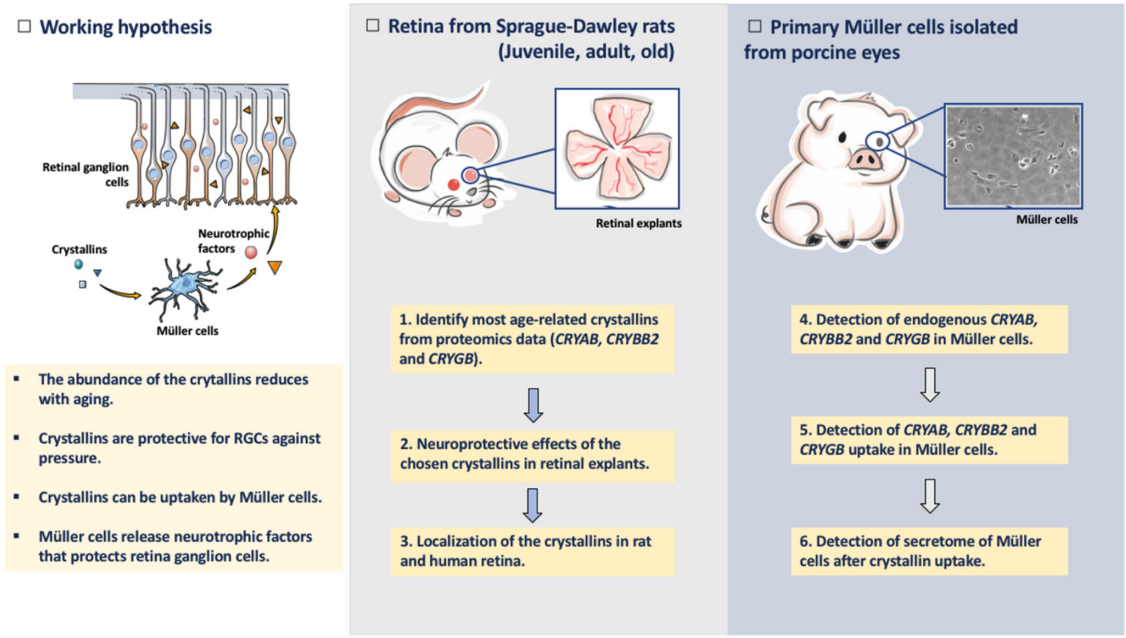

Figure 1. Working hypothesis and workflow overview.

of RGCs. The antibodies were diluted in PBS and spotted in triplicate on a nitrocellulose slide using a non-contact array spotter (Scienion GmbH, Berlin, Germany) to create an antibody microarray. The conditioned medium ($n = 10$ per group) was labeled with Dylight 649 (1:10 in PBS, Thermo Fisher Scientific, Waltham, MA, USA) for 1 hour in the dark and quenched with Tris-HCl for 1 hour. As a negative control, PBS was used. The slides were blocked with 5% BSA in 0.5% Tween-PBS for 1 hour, washed 3 times with 0.5% Tween-PBS, and subsequently incubated with the labeled conditioned medium for 2.5 hours. After washing the slides three times the microarrays were digitalized with an array scanner (Aviso GmbH, Aachen, Germany). For data analysis, spot intensity was quantified with ImaGene 5.0 Software (BioDiscovery, El Segundo, CA, USA). Defective spots were manually excluded from further evaluation. The fluorescence intensities were then determined, with the median signal of the respective triplicates being averaged. Fold-changes of the fluorescence intensities were calculated, a cutoff of 1.5 was used to determine the significantly differentially expressed secretome, as described before.[45–47] The overview of the workflow carried out in this study is presented in Figure 1.

Results

Crystallin Expression in the Glaucoma Model of Chronical Elevated IOP at Different Ages

The results from the mass-spectrometric based approach were statistically evaluated with a special focus on crystallin subtypes known to have an age-related reduction in abundance and potential neuroprotective properties based on literature research and on our own previous findings. In our study, we found these crystallins alpha-crystallin B (*CRYAB*), beta-crystallin B2 (*CRYBB2*), and gamma-crystallin B (*CRYGB*) to be significantly more abundant in the retina of animals in response to chronically elevated IOP and changed throughout aging (Fig. 2) (Supplementary Data S2).

Investigative Ophthalmology & Visual Science

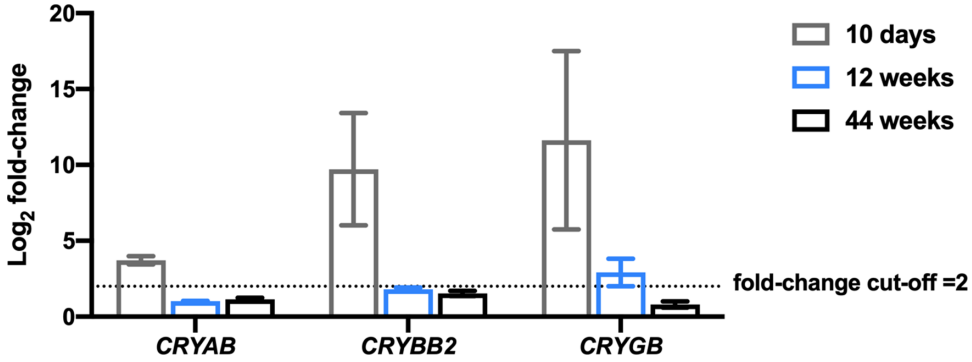

Figure 2. Abundance changes in alpha-crystallin B (*CRYAB*), beta-crystallin B2 (*CRYBB2*), and gamma-crystallin B (*CRYGB*). *CRYAB*, *CRYBB2*, and *CRYGB* show a clear increase in abundance within aging in response to chronically elevated IOP, the increase in the 10-day-old animals is particularly significant. The rate of the increase in all three crystallins decreases with ageing (10 days: $n = 5$, 12 weeks: $n = 7$, and 44 weeks: $n = 5$; vertical bars represented means ± SEM, fold-change cutoff = 2).

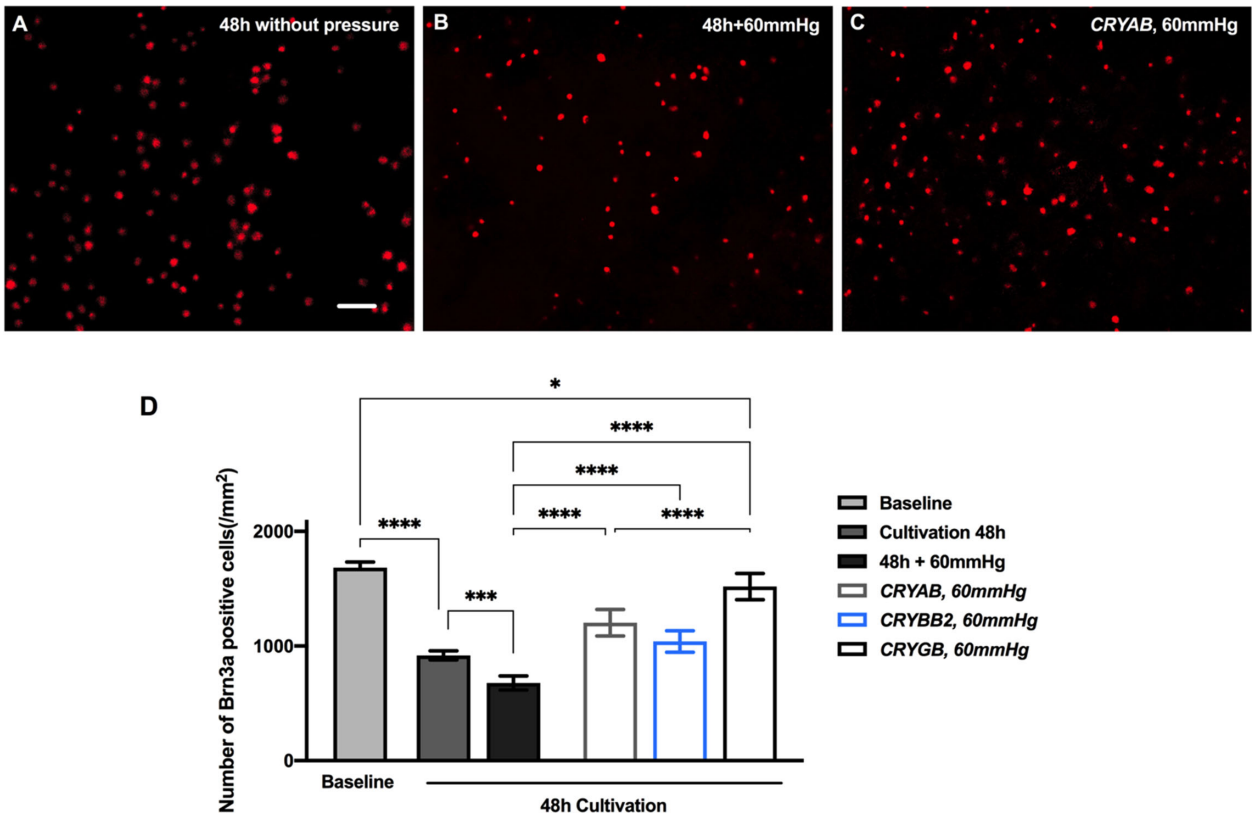

Figure 3. Effects of different crystallins on RGC survival under 60 mm Hg hydrostatic pressure in retina explants in vitro. (**A–C**) Representative fluorescence microscopy of Brn3a staining after 48 hours of cultivation with (**B**) or without (**A**) elevated hydrostatic pressure conditions (60 mm Hg), and with additional *CRYAB* (**C**). (**D**) After 48 hours of cultivation without pressure, it significantly reduced the number of the Brn3a positive RGCs to 918 ± 39.5/mm^2 (****$P < 0.0001$) and an additional 60 mm Hg of hydrostatic pressure further reduced the number of RGC to 678 ± 61.4/mm^2 (***$P < 0.0005$). All three crystallins significantly improved the RGC survival against elevated pressure, whereas *CRYGB* showed the most significant protective effect in vitro.

Neuroprotective Effects of *CRYAB*, *CRYBB2*, and *CRYGB* on Retinal Ganglion Cells In Vitro

The effects of *CRYAB*, *CRYBB2*, and *CRYGB* as being most interesting in part one were selected for this part of the study to further elucidate the mechanism of action in neuroprotection. Representative fluorescence microscopy of Brn3a staining after 48 hours of cultivation with or without elevated hydrostatic pressure conditions (60 mm Hg), and with additional *CRYAB* are given in Figures 3A, 3B, and 3C.

In retinal explants without cultivation (baseline), an average number of 1684/mm^2 was determined. A reduction in RGC numbers to 918 ± 39.5/mm^2 (****$P < 0.0001$) was counted after cultivating the explants in vitro for 48 hours without additional pressure challenge. Additional hydrostatic pressure elevation to 60 mm Hg during the 48 hours

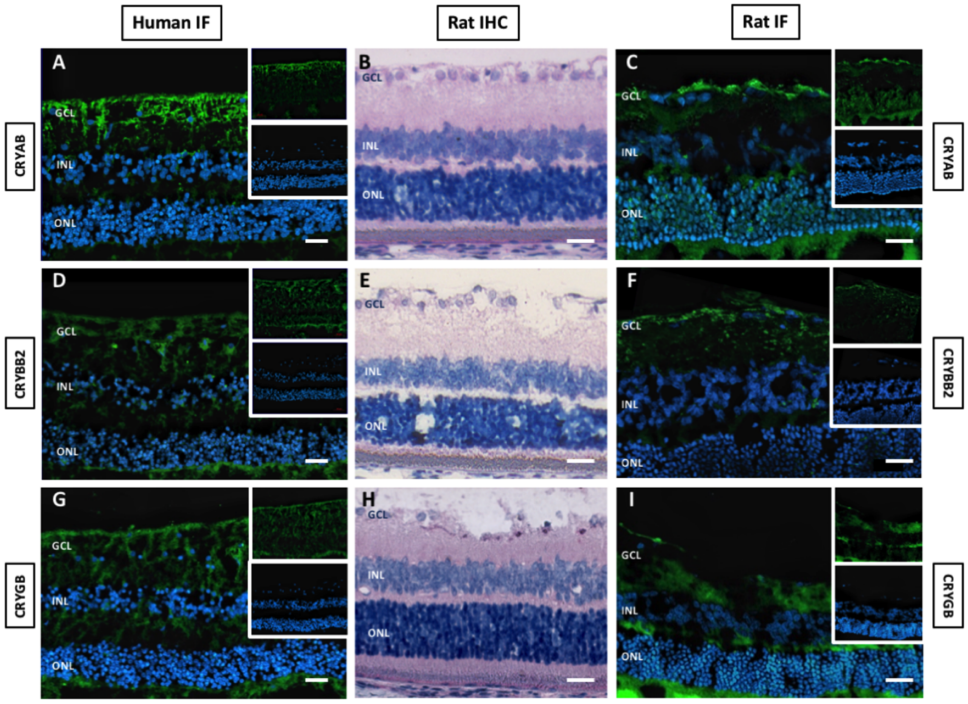

Figure 4. Immunodetection of α-crystallin B (*CRYAB*), β-crystallin B2 (*CRYBB2*), and γ-crystallin B (*CRYGB*) in the retina from humans and Sprague-Dawley rats. The *left panel* shows expression profile of the crystallins in the human retina. The *middle* and *right panels* represent expression profile of the crystallins in the rat retina. Corresponding expression profile of the crystallins can be seen in both human and rat retina. *CRYAB*, *CRYBB2*, and *CRYGB* are expressed in both human and rat retina and is predominantly detected in the ganglion cell layer (GCL) and weakly noted inner nuclear layer (INL) and outer nuclear layer (ONL). In both human and rat retina, immunoreactivity for *CRYGB* is weaker compared to *CRYAB* and *CRYBB2* (scale bars = 20 µm).

of incubation time further reduced the number of RGC to 678 ± 61.4/mm^2 (***P < 0.0005). Incubating the explants with *CRYGB* significantly improved the RGC survival to 1519 ± 115.1/mm^2, *CRYAB* and *CRYBB2* increased the survival to 1203 ± 115/mm^2 and 1040 ± 93.3/mm^2, respectively (Fig. 3D, ****P < 0.0001, ***P < 0.005, and *P < 0.05;

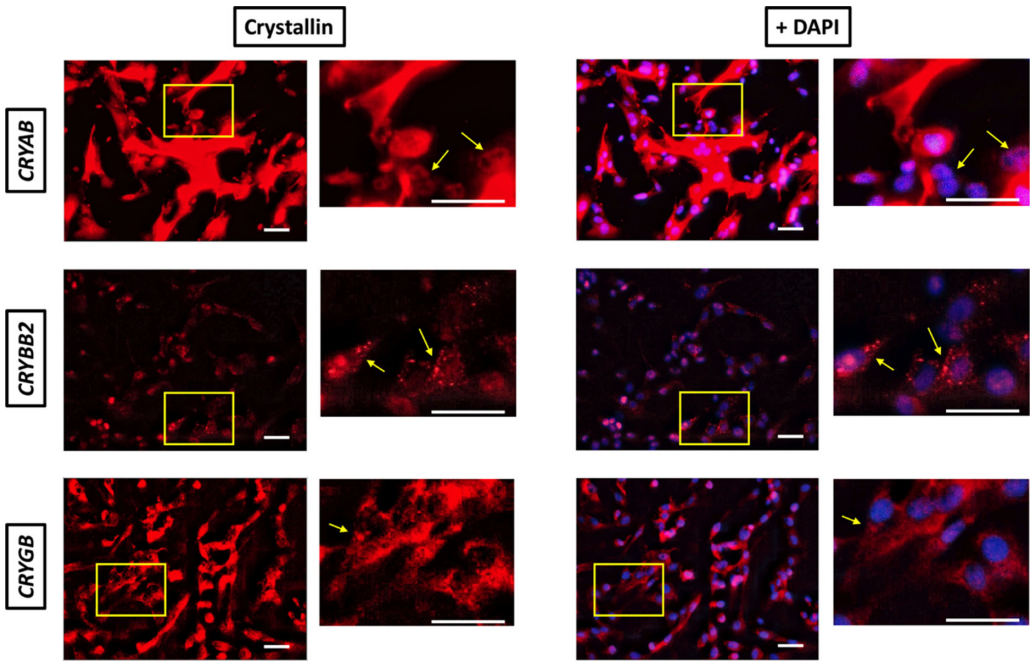

Figure 5. Detection of endogenous crystallin in primary Müller cells. Primary Müller cells were fixed and then stained immunohistochemically against *CRYAB*, *CRYBB2*, and *CRYGB*. Cell nuclei are marked by DAPI (*blue*) and endogenous crystallins are shown in TRITC channel (*red*). All three crystallins can be detected in Müller cells. *CRYAB* showed the strongest fluorescent among all and a distinguishable diffuse distribution pattern throughout the Müller cells. The endogenous *CRYBB2* and *CRYGB* showed weaker fluorescent and are distributed in the cytoplasm.

Investigative Ophthalmology & Visual Science

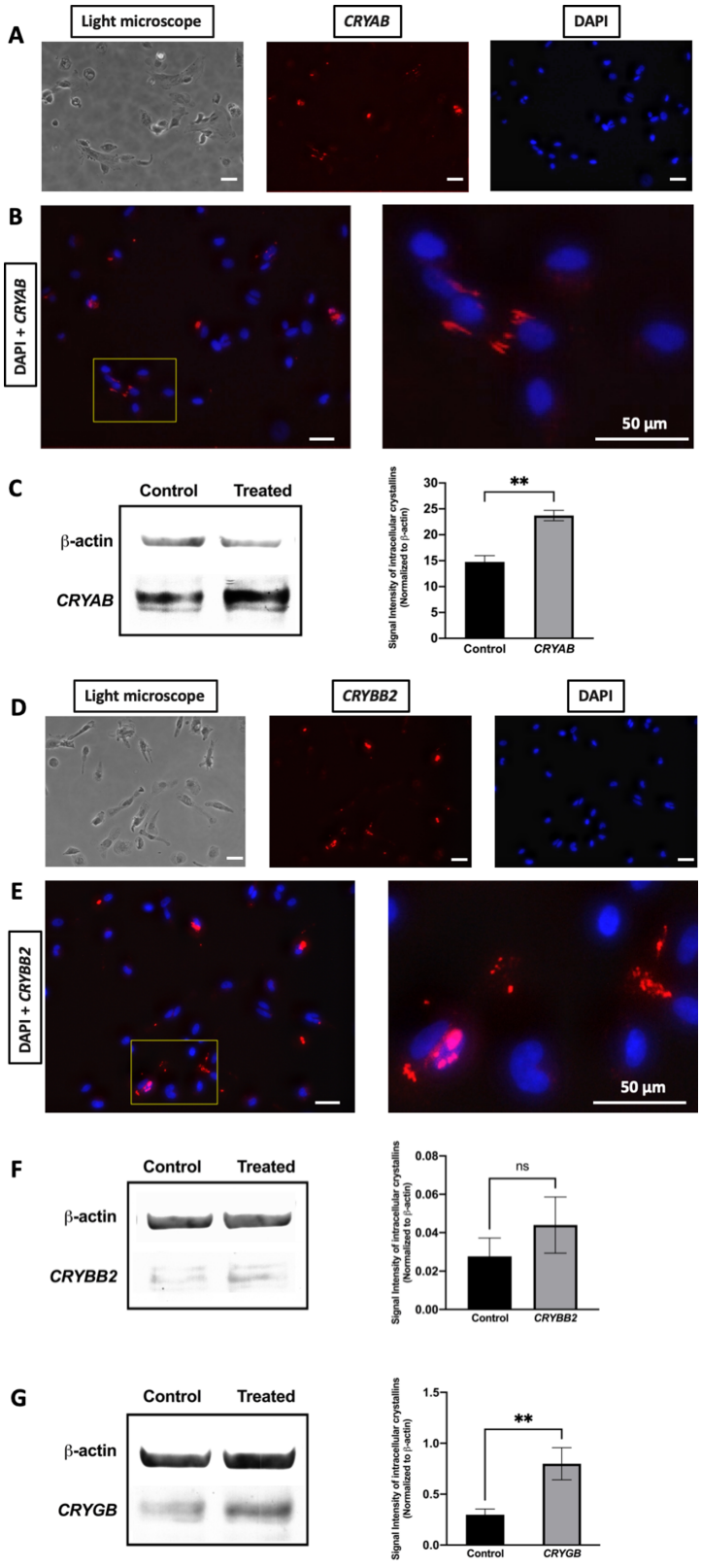

Figure 6. Intracellular uptake of crystallins in primarily isolated Müller cells from pig eyes. (**A, B**) Representative microscopy images of Müller cells incubated with labeled *CRYAB*. (**A**) Müller cells under light microscope, *CRYAB* in the TRITC channel, and cell nuclei in the DAPI channel. (**B**) Merged TRITC and DAPI channels, *CRYAB* can be seen accumulated in cytoplasm around nuclei. (**D, E**) Representative microscopy images of Müller cells incubated with labelled *CRYBB2*. (**A**) Müller cells under light microscope, *CRYBB2* in the TRITC channel, and cell nuclei in the DAPI channel. (**B**) Merged TRITC and DAPI channels, *CRYBB2* can be seen accumulated in cytoplasm around nuclei. (**C, F, G**) The signal intensity of all crystallins are increased in the Müller cells incubated with the respective crystallin. The intracellular abundance of *CRYAB* and *CRYGB* in the Müller cells are both significantly increased compared to the control, whereas the abundance of *CRYBB2* in the Müller cells was not significantly changed (**P <0.01, $n = 3$; vertical bars represent means ± SD; scale bar = 50 µm).

Investigative Ophthalmology & Visual Science

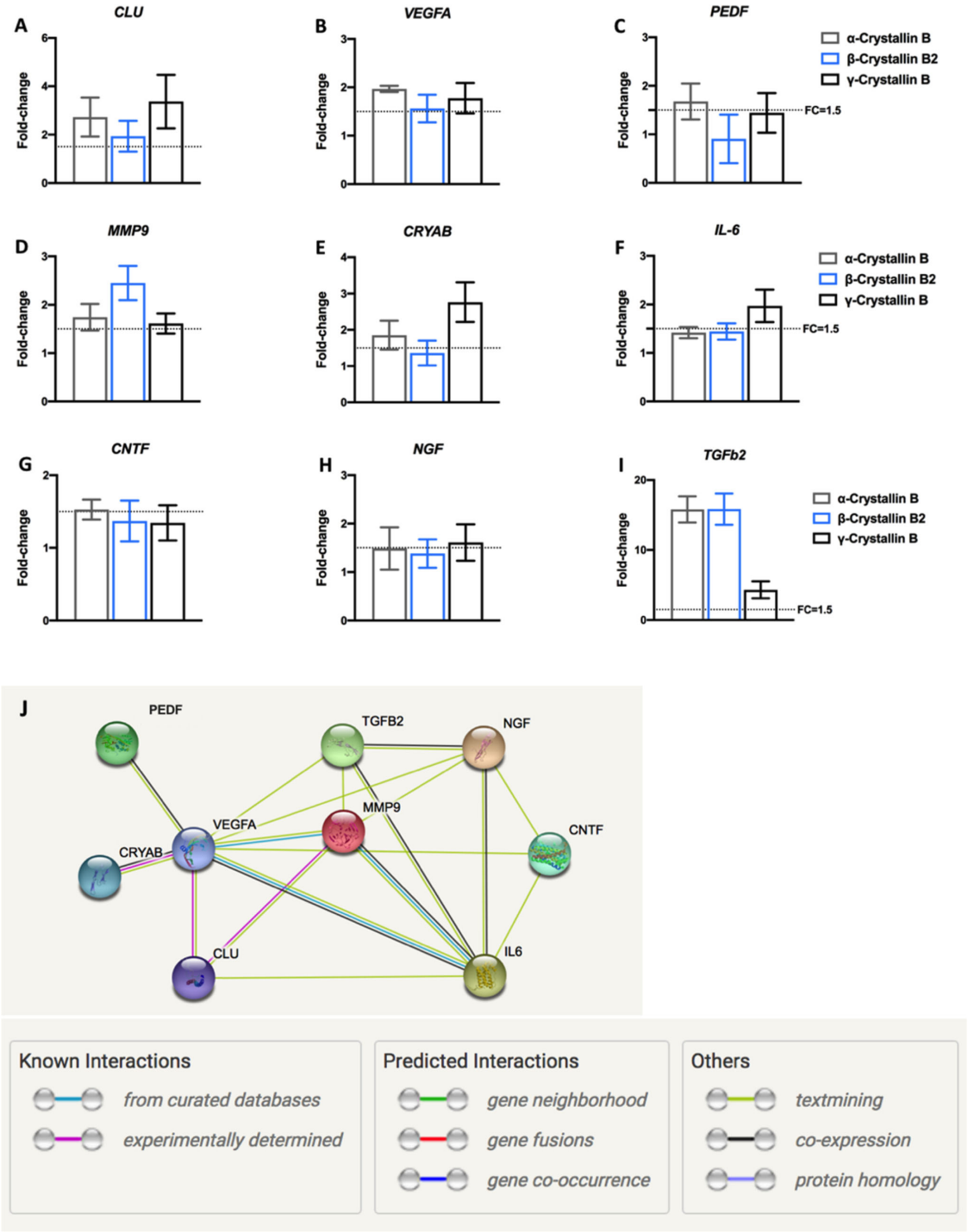

Figure 7. The effect of α-crystallin B (*CRYAB*), β-crystallin B2 (*CRYBB2*), and γ-crystallin B (*CRYGB*) on the secretion of growth factors by primary Müller cells (**A–I**). The charts represent the median signal corresponding to the proteins bound with the dye Cy5. The growth factors *CLU*, *VEGFA*, *MMP9*, *CRYAB*, *IL-6*, *CNTF*, *NGF*, *and TGFb2* are significantly upregulated (fold-change cutoff = 1.5; $n = 5$). (**J**) Protein-protein interaction network (from string-db.org) of the nine genes which are related to the uptake of the crystallins (medium confidence = 0.400).

$n = 6$ quarters of retina/group; vertical bars represented means ± SD).

Immunodetection of Crystallin in Human and Rat Retina

To determine the localization of *CRYAB*, *CRYBB2*, and *CRYGB* in the retina, retinal samples from both human and Sprague-Dawley rats were examined. Crystallins shown similar expression pattern in both human and rat retina. *CRYAB*, *CRYBB2*, and *CRYGB* is predominantly detected in the ganglion cell layer (GCL) and weakly noted inner nuclear layer (INL) and outer nuclear layer (ONL). However, the fluorescence signal of *CRYGB* is weaker compared to *CRYAB* and *CRYBB2* (Fig. 4).

Investigative Ophthalmology & Visual Science

Table 2. Functional Enrichments in Network of Cytokines Upregulated in All Crystallin Groups

GO -Term	Description	Strength	False Discovery Rate	Genes
Biological Process (Gene Ontology)				
GO: 0001974	Blood vessel remodeling	2.56	0.0064	*VEGFA*, *TGFb2*
GO: 0061383	Trabecula morphogenesis	2.54	0.0064	*VEGFA*, *TGFb2*
GO: 0003151	Outflow tract morphogenesis	2.35	0.0072	*VEGFA*, *TGFb2*
GO: 0048771	Tissue remodeling	2.18	0.0038	*VEGFA*, *TGFb2*, *MMP9*
GO: 2001234	Negative regulation of apoptotic signaling pathway	1.93	0.0064	*CLU*, *VEGFA*, *MMP9*

Immunodetection of Endogenous Crystallins in Primary Müller Cells

To detect the endogenous crystallins in Müller cells, primary Müller cells were stained 1 day after passaging, against α-crystallin B (*CRYAB*), β-crystallin B2 (*CRYBB2*), and γ-crystallin B (*CRYGB*) using specific antibodies and the cell nuclei were labeled by DAPI (Fig. 5). All three crystallin were detected in primary Müller cells. Endogenous *CRYAB* has shown the strongest fluorescent and a distinguishing diffuse distribution pattern throughout the cells, whereas the endogenous *CRYBB2* and *CRYGB* have shown weaker fluorescence and were distributed in the cytoplasm (Scale bar = 50 µm).

Intracellular Uptake of Crystallins in Primarily Isolated Müller Cells From Porcine Eyes

Primary Müller cells were incubated for 1 hour with basic medium or with additional *CRYAB*, *CRYBB2*, or *CRYGB* labeled with Mix-n-Stain CF555 Antibody Labeling Kit (Sigma Aldrich, St. Louis, MO, USA). The Müller cells were then washed, fixed, and analyzed by a fluorescence microscope. Müller cells incubated with labeled crystallins showed red fluorescence in scattered areas within the cytoplasm, whereas all cell nuclei were marked by DAPI in blue. Merged images confirm the crystallins were uptaken by Müller cells and accumulated in small vesicles in the cytoplasm around the nuclei (Figs. 6B, 6E).

Furthermore, the uptaken crystallins by Müller cells were quantified by Western blot analysis. The crystallins *CRYAB*, *CRYBB2*, and *CRYGB* could be detected in the control cells as well as in the Müller cells incubated with the different crystallins. The molecular weight (MW) of CRYAB, CRYBB2, and CRYGB are 24 kDa, 23 kDa, and 21 kDa and they were detected in the Western blot at the expected MW (Supplementary Material S3). The signals of the crystallins were set in relation to the charge control and are given below as the relative signal intensity.

An average signal intensity of *CRYAB* is detected at 14.75 $\pm$ 2.14 in the control group and 23.72 $\pm$ 2.01 in the treated sample (**$P < 0.01$, $n = 3$; see Fig. 6C). In accordance with the immunocytochemistry, the signal for CRYBB2 was also weak in the Western blot. The mean signal intensity of the samples incubated with this crystallin (0.044 $\pm$ 0.015) showed a slight but nonsignificant increase in comparison to the control cells (0.028 $\pm$ 0.01, $P = 0.18$, $n = 3$; see Fig. 6F). *CRYGB* was also detected with higher signal intensity in the cells incubated with the crystallin in comparison to control cells (0.7985 $\pm$ 0.158 vs. 0.2979 $\pm$ 0.056; **$P < 0.01$, $n = 3$; see Fig. 6G).

Secretome Analysis by Microarray

The fluorescence intensity of clusterin (*CLU*), *VEGFA*, *MMP9*, and transforming growth factor beta 2 (*TGFb2*) was significantly increased after incubation with *CRYAB*, *CRYBB2*, and *CRYGB*. *TGFb2* showed a more than 15-fold increase in the cells incubated with *CRYAB* and *CRYBB2* (Figs. 7A, 7B, 7D, 7I). Incubation with *CRYGB* increased the secretion of *CRYAB* (Fig. 7E) and *PEDF* is increased in both the cells incubated with *CRYAB* and *CRYGB*. CNTF was exclusively increased in cells incubated with *CRYAB*, whereas *IL-6* and nerve growth factor (*NGF*) were exclusively increased in cells incubated with *CRYGB*. Protein-protein interaction network (from string-db.org) of the nine respective genes of the proteins which are related to the uptake of the crystallins (medium confidence = 0.400; Fig. 7J).

Functional Enrichment in the Network

To get better understanding and insight into the functional role of the crystallin regulated secretome, a functional enrichment analysis by the biological functions (gene ontology [GO]) classification of the differentially crystallin upregulated targets was performed. *CLU*, *VEGFA*, *MMP9*, and *TGFb2* are the proteins with higher abundance in the secretome of cells incubated by all three crystallins. The top GO terms for biological functions of these proteins comprise blood vessel remodeling, trabecula morphogenesis, outflow track morphogenesis, tissue remodeling, and negative regulation of apoptotic signaling pathway (Table 2).

Some proteins were exclusively higher abundant in the secretome of cells incubated with *CRYAB* or *CRYGB*. The respective functional enrichment analyses can be found in Tables 3 and 4. The top GO terms exclusively regulated in the *CRYAB* network are negative regulation of amyloid

Table 3. Enrichment Analysis by Biological Process of *CRYAB*-Regulated Proteins

GO Term	Description	Strength	False Discovery Rate	Genes
Biological Process (Gene Ontology)				
GO: 1905907	Negative regulation of amyloid fibril formation	3.21	0.00071	*CRYAB*, *CLU*
GO: 0061900	Glial cell activation	2.35	0.0050	*CLU*, *CNTF*
GO: 0045773	Positive regulation of axon extension	2.18	0.0086	*VEGFA*, *CNTF*

Investigative Ophthalmology & Visual Science

Table 4. Enrichment Analysis by Biological Process of *CRYGB*-Regulated Proteins

GO Term	Description	Strength	False Discovery Rate	Genes
Biological Process (Gene Ontology)				
GO: 1905907	Negative regulation of amyloid fibril formation	3.1	0.00032	*CRYAB*, *CLU*
GO: 0045429	Positive regulation of nitric oxide biosynthetic process	2.15	0.0060	*CLU*, *IL-6*
GO: 2001243	Negative regulation of intrinsic apoptotic signaling pathway	2.08	0.0003	*CLU*, *NGF*, *MMP9*
GO: 0048771	Tissue remodeling	2.05	2.42e-0.5	*IL-6*, *VEGFA*, *MMP9*

fibril formation, glial cell activation, and positive regulation of axon extension. In the *CRYGB* network, the top exclusively regulated GO terms are negative regulation of amyloid fibril formation, positive regulation of nitric oxide biosynthetic process, and negative regulation of intrinsic apoptotic signaling pathway.

Discussion

The data obtained in this study provides further evidence for a potential age-related and also neuroprotective effect of *CRYAB*, *CRYBB2*, and *CRYGB*. The protective effect of crystallins could be mediated by potential endocytotic uptake and involvement of Müller cells in a precise mode of action for each selected crystalline member, respectively.

In the animal model used in this study, it leads to glaucomatous injury, going along with loss of RGCs and their axons, thinning of the retinal nerve fiber layer (RNFL) and functional changes.[6,7] In the presented study, crystallins of all subclasses were found with higher abundance in retinal samples of juvenile animals in response to IOP, whereas the upregulation of crystallins was less distinctive in adult animals and almost entirely lost in the aged animal group. The ability of increasing endogenous crystallin expression might therefore decrease throughout aging, correlated with an age-related increase of RGC susceptibility to IOP. *CRYAB*, *CRYBB2*, and *CRYGB* were mostly significantly correlated with aging.

CRYAB, *CRYBB2*, and *CRYGB* addition to culture reduced RGC loss against elevated pressure in vitro. Neuroprotective effects of *CRYAB* and *CRYBB2* on RGCs in glaucoma animal models has been previously described,[6,7] and *CRYBB2* additionally also demonstrated axonal regeneration properties after optic nerve injury (ONI).[8] Comparing staining for *CRYAB*, *CRYBB2*, and *CRYGB* in human and rat retina, we had a similar expression profile in human and rat retina that was found, although the human staining was of significantly worse quality. The GCL showed the most intense crystallin staining, weaker staining was found in the INL and ONL. Müller cells are the principal glial cells of the retina with an extended funnel shape, radiating from the soma in the inner nuclear layer.[48] We showed that the crystallins are expressed endogenously in primary Müller cells.

Müller cells support the function and metabolism of retinal neurons and are active players in normal retinal function and retinal degeneration.[49] Müller cells provide trophic substances to neurons and remove metabolic waste[50] and can be considered a major contributor to the retinal secretome. Secreted trophic factors are key to maintain the structural and functional integrity of the retinal neurons, as well as mediating inflammatory responses in the retina.[51,52] They regulate synaptic activity through neurotransmitter uptake and recycling, and providing neurons with neurotransmitter precursors.[53] The factors secreted by Müller cells, such as *CNTF*, *BDNF*, *ApoE*, *CLU*, and *PEDF*,[33,54,55] exert beneficial effects on survival of RGCs and neurite regeneration in vitro and may constitute effective agents for neuroprotection of RGC.[56]

We showed that external crystallins, especially *CRYAB* and *CRYGB*, can be incorporated into the cytoplasmic space of Müller cells, which went in hand with an increased secretion of *CLU*, *VEGFA*, *MMP9*, and *TGFb2*. The most obvious increase of secretion was detected for *TGFb2*.

TGFb2 is a secreted protein known as a multifunctional cytokine with important implications in morphogenesis, cell differentiation, and tissue remodeling,[57] as well as an important regulator of neuronal survival. Although it is not neurotrophic itself, *TGFb2* can drastically increase the potency of neurotrophins, such as fibroblast growth factor-2, *CNTF*, and glial cell line-derived neurotrophic factor.[58] Furthermore, *CLU*, *VEGFA*, and *MMP9* have all shown neuroprotective potentials.

Clusterin plays a prosurvival role during cell death and confers resistance against cytotoxic agents.[59,60] Upregulation of *CLU* is documented in neuronal injuries and degenerations, including Alzheimer's disease, spinal cord injury, neovascular age-related macular degeneration, and retinal degeneration induced by ischemia, diabetes, and light.[61–69]

VEGFA has recently been recognized as an important neuroprotectant in the central nervous system (CNS), it has been shown to influence not only the maintenance of the normal vasculature but also neuronal growth, maintenance, and survival.[70–72] Within the context of the retina, the receptors for *VEGFA* are present in normal retinal neuronal cells and RGCs were found to be exquisitely sensitive to *VEGFA* depletion compared with other tissues.[70,73,74] Depressed *VEGFA* levels directly impact RGC survival.[70]

The expression of several *MMPs* is altered in patients with glaucoma and in experimental animal models.[75–77] The *MMP9* is a secreted gelatinase,[78] which can cleave inflammatory cytokines, and may modify cytokine signaling during the injury-induced proliferation.[79,80]

The secretion of *CRYAB* and *PEDF* from Müller cells is significantly increased by both *CRYAB* and *CRYGB*. It is impossible to tell if the *CRYAB* in the culture medium of the primary Müller cells incubated with *CRYAB* is the residual of added *CRYAB* or the actual secretion from Müller cells. The expression of *CRYAB* was also increased in the rod outer segments and the retinal pigment epithelium in light induced retinal degeneration,[81,82] as well as in the retina upon glaucomatous injury and mechanical injury.[83,84] As alpha-crystallins demonstrate a chaperone-like activity upon external stimulus,[20–23] and we have shown in this study the strong expression in *CRYAB* in primary Müller cells, it is

Investigative Ophthalmology & Visual Science

reasonable to assume that Müller cells regularly contain a sufficient intracellular pool of *CRYAB*, and is able to release it upon stress stimulus. In addition, interestingly *CRYGB* seems to be one of the regulator of *CRYAB* secretion from Müller cells.

PEDF is a multifunctional protein, besides its demonstrable neurotrophic action, *PEDF* also exhibits antiangiogenic activity, such as inhibition of retinal and choroidal neovascularization.[85,86] In mice, murine, and human retina, a reduced *PEDF* level is correlated with retinal degeneration.[87–90]

Furthermore, *CNTF* is a well-known neurotrophic factor secreted by retinal Müller cells.[36] Crystallins seem to upregulate the expression of *CNTF*.[31,32] In this study, significant upregulation of *CNTF* is seen exclusively in the *CRYAB* group.

In the *CRYGB* group, *NGF* and *IL-6* are significantly increased. *NGF* is a polypeptide member of the small family of evolutionarily well-conserved neurotrophins, such as BDNF and neurotrophin-3 (NT3).[91] Increased availability of mature *NGF* is shown to improve RGC survival and axonal growth.[92–95]

IL-6 is involved in a variety of the CNS pathologies, including injury, infection, and neurodegeneration.[96] The effect of *IL6* on neuronal health is variable. In the retina of rodent glaucoma models, *IL-6* and its mRNA are upregulated surrounding the RGCs and their axons.[97–100] Application of *IL-6* protects cultured RGCs from pressure-induced apoptosis[101,102] and promotes axon regeneration following optic nerve crush.[103,104] There are also studies suggesting that *IL-6* deficiency protects RGCs in models of glutamate excitotoxicity and optic nerve crush[105] and prevents both structural degeneration of the optic nerve and vision loss in a high-IOP glaucoma model in mice.[106]

There are some limitations in the present study we would like to highlight. First, in the exploratory proteomics experiment, contralateral eyes of the animals were used as control to reduce the number of the animals in this study. The contralateral eyes are not always the perfect control group due to sympathetic inflammatory responses in the eyes. As we were looking at the changes in the crystallins, the abundance of the crystallins in the contralateral eyes would likely alter in the same direction, thus leading to a less significant result over all. Therefore, using the contralateral eye as the control does not influence this study. Second, it is always beneficial to use more than one technique to reconfirm the findings from label-free quantification. Due to the limitation of sample material and the plethora isoforms of crystallin, we cannot confirm all differentially expressed crystallins by a second technique in the present study design. The main focus of this study was to explore the neuroprotective effects of crystallins and the underlying mechanism. Building on these results, different techniques will be used to further study the crystallins' role in aging and glaucoma. Last, but not least, it is unlikely that all the proteins responsible for the neuroprotective effects of the Müller cells are identified by means of microarray analysis. We also tried to analyze the Müller cell secretome via mass-spectrometry assisted proteomics approaches, unfortunately, due to the masking effect of albumin, which is highly abundant in culture medium, we failed to identify the low-abundant proteins in the culture medium (Supplementary Data S4). Although, the most significantly increased proteins are proven to play positive roles in the survival and regeneration of RGCs, the exact roles of the significantly increased proteins in RGC degeneration remain to be elucidated.

To summarize, we found in this study, that *CRYAB*, *CRYBB2*, and *CRYGB* are most significantly correlated with aging in an experimental animal model of glaucoma. All three of them are neuroprotective of RGCs against elevated hydrostatic pressure in vitro. Crystallins are expressed endogenously in primary Müller cells. Furthermore, all crystallins can be uptaken by Müller cells, the uptake of *CRYAB* and *CRYGB* is statistically significant. Uptake of *CRYAB*, *CRYBB2*, and *CRYGB* led to different patterns of increase secretion of neurotrophic factors. Future studies are needed to go into more details into the involved signaling pathways and modes of action.

Acknowledgments

The authors thank Rodica-Aurelia Maniu for technical assistance.

Funded by Deutsche Forschungsgemeinschaft PR 1569 1/1 and PR 1569 1/3, AECOS 2014.

Disclosure: **H. Liu**, None; **K. Bell**, None; **A. Herrmann**, None; **S. Arnhold**, None; **K. Mercieca**, None; **F. Anders**, None; **K. Nagel-Wolfrum**, None; **S. Thanos**, None; **V. Prokosch**, None

References

1. Weinreb RN, Aung T, Medeiros FA. The pathophysiology and treatment of glaucoma: a review. *JAMA*. 2014;311:1901–1911.
2. Cockburn DM. Does reduction of intraocular pressure (IOP) prevent visual field loss in glaucoma? *Am J Optom Physiologic Optics*. 1983;60:705–711.
3. Trautner C, Haastert B, Richter B, Berger M, Giani G. Incidence of blindness in southern Germany due to glaucoma and degenerative conditions. *Invest Ophthalmol Vis Sci*. 2003;44:1031–1034.
4. Quigley HA, Broman AT. The number of people with glaucoma worldwide in 2010 and 2020. *Br J Ophthalmol*. 2006;90:262–267.
5. Anders F, Mann C, Liu A, et al. Correlation of Crystallin Expression and RGC Susceptibility in Experimental Glaucoma Rats of Different Ages. *Curr Eye Res*. 2018;43:1267–1273.
6. Anders F, Liu A, Mann C, et al. The Small Heat Shock Protein alpha-Crystallin B Shows Neuroprotective Properties in a Glaucoma Animal Model. *Int J Mol Sci*. 2017;18(11):2418.
7. Anders F, Teister J, Liu A, et al. Intravitreal injection of beta-crystallin B2 improves retinal ganglion cell survival in an experimental animal model of glaucoma. *PLoS One*. 2017;12:e0175451.
8. Bohm MR, Prokosch V, Bruckner M, Pfrommer S, Melkonyan H, Thanos S. betaB2-Crystallin Promotes Axonal Regeneration in the Injured Optic Nerve in Adult Rats. *Cell Transplant*. 2015;24:1829–1844.
9. de Jong WW, Hendriks W, Mulders JW, Bloemendal H. Evolution of eye lens crystallins: the stress connection. *Trends in Biochem Sci*. 1989;14:365–368.
10. Wistow G. The human crystallin gene families. *Human Genom*. 2012;6:26.
11. Andley UP. Crystallins in the eye: Function and pathology. *Progress Retinal Eye Res*. 2007;26:78–98.
12. Chen W, Lu Q, Lu L, Guan H. Increased levels of alphaB-crystallin in vitreous fluid of patients with proliferative diabetic retinopathy and correlation with vascular endothelial growth factor. *Clin Exp Ophthalmol*. 2017;45:379–384.

13. Renkawek K, Voorter CE, Bosman GJ, van Workum FP, de Jong WW. Expression of alpha B-crystallin in Alzheimer's disease. *Acta Neuropathologica*. 1994;87:155–160.
14. Prokosch V, Schallenberg M, Thanos S. Crystallins are regulated biomarkers for monitoring topical therapy of glaucomatous optic neuropathy. *PLoS One*. 2013;8:e49730.
15. Piri N, Kwong JM, Caprioli J. Crystallins in retinal ganglion cell survival and regeneration. *Molec Neurobiol*. 2013;48:819–828.
16. Dong Z, Kase S, Ando R, et al. AlphaB-crystallin expression in epiretinal membrane of human proliferative diabetic retinopathy. *Retina*. 2012;32:1190–1196.
17. Hong Y, Zhao T, Li XJ, Li S. Mutant Huntingtin Inhibits alphaB-Crystallin Expression and Impairs Exosome Secretion from Astrocytes. *J Neurosci*. 2017;37:9550–9563.
18. Zhu Z, Reiser G. The small heat shock proteins, especially HspB4 and HspB5 are promising protectants in neurodegenerative diseases. *Neurochemistry Intl*. 2018;115:69–79.
19. Lim EF, Nakanishi ST, Hoghooghi V, et al. AlphaB-crystallin regulates remyelination after peripheral nerve injury. *Proc Natl Acad Sci USA*. 2017;114:E1707–E1716.
20. Derham BK, Harding JJ. Alpha-crystallin as a molecular chaperone. *Prog Retinal Eye Res*. 1999;18:463–509.
21. Horwitz J. Alpha-crystallin can function as a molecular chaperone. *Proc Natl Acad Sci USA*. 1992;89:10449–10453.
22. de Jong WW, Leunissen JA, Voorter CE. Evolution of the alpha-crystallin/small heat-shock protein family. *Molec Biol Evolution*. 1993;10:103–126.
23. Mao YW, Liu JP, Xiang H, Li DW. Human alphaA- and alphaB-crystallins bind to Bax and Bcl-X(S) to sequester their translocation during staurosporine-induced apoptosis. *Cell Death and Differentiation*. 2004;11:512–526.
24. Thanos S, Bohm MR, Meyer zu Horste M, et al. Role of crystallins in ocular neuroprotection and axonal regeneration. *Prog Retin Eye Res*. 2014;42:145–161.
25. Bohm MR, Pfrommer S, Chiwitt C, Bruckner M, Melkonyan H, Thanos S. Crystallin-beta-b2-overexpressing NPCs support the survival of injured retinal ganglion cells and photoreceptors in rats. *Invest Ophthalmol Vis Sci*. 2012;53:8265–8279.
26. Chiu K, Zhou Y, Yeung SC, et al. Up-regulation of crystallins is involved in the neuroprotective effect of wolfberry on survival of retinal ganglion cells in rat ocular hypertension model. *J Cell Biochem*. 2010;110:311–320.
27. Renkawek K, Stege GJ, Bosman GJ. Dementia, gliosis and expression of the small heat shock proteins hsp27 and alpha B-crystallin in Parkinson's disease. *Neuroreport*. 1999;10:2273–2276.
28. Bajramovic JJ, Lassmann H, van Noort JM. Expression of alphaB-crystallin in glia cells during lesional development in multiple sclerosis. *J Neuroimmunol*. 1997;78:143–151.
29. Fort PE, Freeman WM, Losiewicz MK, Singh RS, Gardner TW. The retinal proteome in experimental diabetic retinopathy: up-regulation of crystallins and reversal by systemic and periocular insulin. *Molec Cell Proteomics: MCP*. 2009;8:767–779.
30. Nath M, Shan Y, Myers AM, Fort PE. HspB4/alphaA-Crystallin Modulates Neuroinflammation in the Retina via the Stress-Specific Inflammatory Pathways. *J Clin Med*. 2021;10(11):2384.
31. Fischer D, Hauk TG, Muller A, Thanos S. Crystallins of the beta/gamma-superfamily mimic the effects of lens injury and promote axon regeneration. *Molec Cell Neurosci*. 2008;37:471–479.
32. Hauk TG, Muller A, Lee J, Schwendener R, Fischer D. Neuroprotective and axon growth promoting effects of intraocular inflammation do not depend on oncomodulin or the presence of large numbers of activated macrophages. *Exp Neurol*. 2008;209:469–482.
33. Vecino E, Rodriguez FD, Ruzafa N, Pereiro X, Sharma SC. Glia-neuron interactions in the mammalian retina. *Prog Retin Eye Res*. 2016;51:1–40.
34. Pereiro X, Miltner AM, La Torre A, Vecino E. Effects of Adult Muller Cells and Their Conditioned Media on the Survival of Stem Cell-Derived Retinal Ganglion Cells. *Cells*. 2020;9(8):1759.
35. Goureau O, Rhee KD, Yang XJ. Ciliary neurotrophic factor promotes muller glia differentiation from the postnatal retinal progenitor pool. *Dev Neurosci*. 2004;26:359–370.
36. Seki M, Tanaka T, Sakai Y, et al. Muller Cells as a source of brain-derived neurotrophic factor in the retina: noradrenaline upregulates brain-derived neurotrophic factor levels in cultured rat Muller cells. *Neurochem Res*. 2005;30:1163–1170.
37. Shareef SR, Garcia-Valenzuela E, Salierno A, Walsh J, Sharma SC. Chronic ocular hypertension following episcleral venous occlusion in rats. *Exp Eye Res*. 1995;61:379–382.
38. Liu H, Perumal N, Manicam C, Mercieca K, Prokosch V. Proteomics Reveals the Potential Protective Mechanism of Hydrogen Sulfide on Retinal Ganglion Cells in an Ischemia/Reperfusion Injury Animal Model. *Pharmaceuticals (Basel)*. 2020;13(9):213.
39. Schmelter C, Funke S, Treml J, et al. Comparison of Two Solid-Phase Extraction (SPE) Methods for the Identification and Quantification of Porcine Retinal Protein Markers by LC-MS/MS. *Int J Mol Sci*. 2018;19(12):3847.
40. Cox J, Mann M. MaxQuant enables high peptide identification rates, individualized p.p.b.-range mass accuracies and proteome-wide protein quantification. *Nature Biotechnol*. 2008;26:1367–1372.
41. Brockhaus K, Melkonyan H, Prokosch-Willing V, Liu H, Thanos S. Alterations in Tight- and Adherens-Junction Proteins Related to Glaucoma Mimicked in the Organotypically Cultivated Mouse Retina Under Elevated Pressure. *Invest Ophthalmol Vis Sci*. 2020;61:46.
42. Nadal-Nicolas FM, Sobrado-Calvo P, Jimenez-Lopez M, Vidal-Sanz M, Agudo-Barriuso M. Long-Term Effect of Optic Nerve Axotomy on the Retinal Ganglion Cell Layer. *Invest Ophthalmol Vis Sci*. 2015;56:6095–6112.
43. Nadal-Nicolas FM, Salinas-Navarro M, Jimenez-Lopez M, et al. Displaced retinal ganglion cells in albino and pigmented rats. *Front Neuroanatomy*. 2014;8:99.
44. Bell K, Wilding C, Funke S, et al. Neuroprotective effects of antibodies on retinal ganglion cells in an adolescent retina organ culture. *J Neurochem*. 2016;139:256–269.
45. Boehm N, Wolters D, Thiel U, et al. New insights into autoantibody profiles from immune privileged sites in the eye: a glaucoma study. *Brain, Behavior, Immunity*. 2012;26:96–102.
46. Lorenz K, Beck S, Keilani MM, Wasielica-Poslednik J, Pfeiffer N, Grus FH. Longitudinal Analysis of Serum Autoantibody-Reactivities in Patients with Primary Open Angle Glaucoma and Optic Disc Hemorrhage. *PLoS One*. 2016;11:e0166813.
47. Bohm D, Keller K, Boehm N, et al. Antibody microarray analysis of the serum proteome in primary breast cancer patients. *Cancer Biol Ther*. 2011;12:772–779.
48. Newman E, Reichenbach A. The Muller cell: a functional element of the retina. *Trends Neurosci*. 1996;19:307–312.
49. Bringmann A, Pannicke T, Grosche J, et al. Muller cells in the healthy and diseased retina. *Prog Retin Eye Res*. 2006;25:397–424.
50. Tsacopoulos M, Magistretti PJ. Metabolic coupling between glia and neurons. *J Neurosci*. 1996;16:877–885.
51. Araujo RS, Santos DF, Silva GA. The role of the retinal pigment epithelium and Muller cells secretome in neovascular retinal pathologies. *Biochimie*. 2018;155:104–108.

Investigative Ophthalmology & Visual Science

52. Hauck SM, von Toerne C, Ueffing M. The neuroprotective potential of retinal Muller glial cells. *Adv Exp Med Biol*. 2014;801:381–387.
53. Pereiro X, Ruzafa N, Acera A, Urcola A, Vecino E. Optimization of a Method to Isolate and Culture Adult Porcine, Rats and Mice Muller Glia in Order to Study Retinal Diseases. *Front Cell Neurosci*. 2020;14:7.
54. Ruzafa N, Pereiro X, Lepper MF, Hauck SM, Vecino E. A Proteomics Approach to Identify Candidate Proteins Secreted by Muller Glia that Protect Ganglion Cells in the Retina. *Proteomics*. 2018;18:e1700321.
55. Unterlauft JD, Claudepierre T, Schmidt M, et al. Enhanced survival of retinal ganglion cells is mediated by Muller glial cell-derived PEDF. *Exp Eye Res*. 2014;127:206–214.
56. Garcia M, Forster V, Hicks D, Vecino E. Effects of muller glia on cell survival and neuritogenesis in adult porcine retina in vitro. *Invest Ophthalmol Vis Sci*. 2002;43:3735–3743.
57. Clark DA, Coker R. Transforming growth factor-beta (TGF-beta). *Intl J Biochem Cell Biol*. 1998;30:293–298.
58. Krieglstein K, Strelau J, Schober A, Sullivan A, Unsicker K. TGF-beta and the regulation of neuron survival and death. *J Physiol Paris*. 2002;96:25–30.
59. Shannan B, Seifert M, Leskov K, et al. Challenge and promise: roles for clusterin in pathogenesis, progression and therapy of cancer. *Cell Death and Differentiation*. 2006;13:12–19.
60. Trougakos IP, Gonos ES. Regulation of clusterin/apolipoprotein J, a functional homologue to the small heat shock proteins, by oxidative stress in ageing and age-related diseases. *Free Radical Res*. 2006;40:1324–1334.
61. May PC, Finch CE. Sulfated glycoprotein 2: new relationships of this multifunctional protein to neurodegeneration. *Trends in Neurosci*. 1992;15:391–396.
62. Klimaschewski L, Obermuller N, Witzgall R. Regulation of clusterin expression following spinal cord injury. *Cell Tissue Res*. 2001;306:209–216.
63. Liu L, Svensson M, Aldskogius H. Clusterin upregulation following rubrospinal tract lesion in the adult rat. *Expl Neurol*. 1999;157:69–76.
64. Wong P, Borst DE, Farber D, et al. Increased TRPM-2/clusterin mRNA levels during the time of retinal degeneration in mouse models of retinitis pigmentosa. *Biochem Cell Biol*. 1994;72:439–446.
65. Gwon JS, Kim IB, Lee MY, Oh SJ, Chun MH. Expression of clusterin in Muller cells of the rat retina after pressure-induced ischemia. *Glia*. 2004;47:35–45.
66. Zhou M, Shen D, Head JE, et al. Ocular clusterin expression in von Hippel-Lindau disease. *Molec Vis*. 2007;13:2129–2136.
67. Kim YS, Kim YH, Cheon EW, et al. Retinal expression of clusterin in the streptozotocin-induced diabetic rat. *Brain Res*. 2003;976:53–59.
68. Wong P, Ulyanova T, Organisciak DT, et al. Expression of multiple forms of clusterin during light-induced retinal degeneration. *Curr Eye Res*. 2001;23:157–165.
69. Nobl M, Reich M, Dacheva I, et al. Proteomics of vitreous in neovascular age-related macular degeneration. *Expl Eye Res*. 2016;146:107–117.
70. Nishijima K, Ng YS, Zhong L, et al. Vascular endothelial growth factor-A is a survival factor for retinal neurons and a critical neuroprotectant during the adaptive response to ischemic injury. *Am J Pathol*. 2007;171:53–67.
71. Jin KL, Mao XO, Greenberg DA. Vascular endothelial growth factor: direct neuroprotective effect in in vitro ischemia. *Proc Natl Acad Sci USA*. 2000;97:10242–10247.
72. Sondell M, Sundler F, Kanje M. Vascular endothelial growth factor is a neurotrophic factor which stimulates axonal outgrowth through the flk-1 receptor. *Eur J Neurosci*. 2000;12:4243–4254.
73. Yang X, Cepko CL. Flk-1, a receptor for vascular endothelial growth factor (VEGF), is expressed by retinal progenitor cells. *J Neurosci*. 1996;16:6089–6099.
74. Kim I, Ryan AM, Rohan R, et al. Constitutive expression of VEGF, VEGFR-1, and VEGFR-2 in normal eyes. *Invest Ophthalmol Vis Sci*. 1999;40:2115–2121.
75. Agapova OA, Ricard CS, Salvador-Silva M, Hernandez MR. Expression of matrix metalloproteinases and tissue inhibitors of metalloproteinases in human optic nerve head astrocytes. *Glia*. 2001;33:205–216.
76. Agapova OA, Kaufman PL, Lucarelli MJ, Gabelt BT, Hernandez MR. Differential expression of matrix metalloproteinases in monkey eyes with experimental glaucoma or optic nerve transection. *Brain Res*. 2003;967:132–143.
77. Yan X, Tezel G, Wax MB, Edward DP. Matrix metalloproteinases and tumor necrosis factor alpha in glaucomatous optic nerve head. *Arch Ophthalmol*. 2000;118:666–673.
78. Masure S, Proost P, Van Damme J, Opdenakker G. Purification and identification of 91-kDa neutrophil gelatinase. Release by the activating peptide interleukin-8. *Eur J Biochem*. 1991;198:391–398.
79. Parks WC, Wilson CL, Lopez-Boado YS. Matrix metalloproteinases as modulators of inflammation and innate immunity. *Nat Rev Immunol*. 2004;4:617–629.
80. Ando K, Shibata E, Hans S, Brand M, Kawakami A. Osteoblast Production by Reserved Progenitor Cells in Zebrafish Bone Regeneration and Maintenance. *Develop Cell*. 2017;43:643–650.e643.
81. Sakaguchi H, Miyagi M, Darrow RM, et al. Intense light exposure changes the crystallin content in retina. *Exp Eye Res*. 2003;76:131–133.
82. Organisciak D, Darrow R, Gu X, Barsalou L, Crabb JW. Genetic, age and light mediated effects on crystallin protein expression in the retina. *Photochemistry Photobiol*. 2006;82:1088–1096.
83. Vazquez-Chona F, Song BK, Geisert EE, Jr. Temporal changes in gene expression after injury in the rat retina. *Invest Ophthalmol Vis Sci*. 2004;45:2737–2746.
84. Steele MR, Inman DM, Calkins DJ, Horner PJ, Vetter ML. Microarray analysis of retinal gene expression in the DBA/2J model of glaucoma. *Invest Ophthalmol Vis Sci*. 2006;47:977–985.
85. Bouck N. PEDF: anti-angiogenic guardian of ocular function. *Trends Mol Med*. 2002;8:330–334.
86. Craword SE, Fitchev P, Veliceasa D, Volpert OV. The many facets of PEDF in drug discovery and disease: a diamond in the rough or split personality disorder? *Expert Opin Drug Discov*. 2013;8:769–792.
87. Hernandez-Pinto A, Polato F, Subramanian P, et al. PEDF peptides promote photoreceptor survival in rd10 retina models. *Exp Eye Res*. 2019;184:24–29.
88. Wang Y, Subramanian P, Shen D, Tuo J, Becerra SP, Chan CC. Pigment epithelium-derived factor reduces apoptosis and pro-inflammatory cytokine gene expression in a murine model of focal retinal degeneration. *ASN Neuro*. 2013;5:e00126.
89. Holekamp NM, Bouck N, Volpert O. Pigment epithelium-derived factor is deficient in the vitreous of patients with choroidal neovascularization due to age-related macular degeneration. *Am J Ophthalmol*. 2002;134:220–227.
90. Ogata N, Matsuoka M, Imaizumi M, Arichi M, Matsumura M. Decreased levels of pigment epithelium-derived factor in eyes with neuroretinal dystrophic diseases. *Am J Ophthalmol*. 2004;137:1129–1130.
91. Huang EJ, Reichardt LF. Neurotrophins: roles in neuronal development and function. *Ann Rev Neurosci*. 2001;24:677–736.

Investigative Ophthalmology & Visual Science

92. Mesentier-Louro LA, Rosso P, Carito V, et al. Nerve Growth Factor Role on Retinal Ganglion Cell Survival and Axon Regrowth: Effects of Ocular Administration in Experimental Model of Optic Nerve Injury. *Molec Neurobiol*. 2019;56:1056–1069.
93. Turner JE, Delaney RK. Retinal ganglion cell response to axotomy and nerve growth factor antiserum in the regenerating visual system of the newt (Notophthalmus viridescens): an ultrastructural morphometric analysis. *Brain Res*. 1979;177:35–47.
94. Yip HK, Johnson EM, Jr. Retrograde transport of nerve growth factor in lesioned goldfish retinal ganglion cells. *J Neurosci*. 1983;3:2172–2182.
95. Carmignoto G, Maffei L, Candeo P, Canella R, Comelli C. Effect of NGF on the survival of rat retinal ganglion cells following optic nerve section. *J Neurosci*. 1989;9:1263–1272.
96. Erta M, Quintana A, Hidalgo J. Interleukin-6, a major cytokine in the central nervous system. *Int J Biol Sci*. 2012;8:1254–1266.
97. Sappington RM, Calkins DJ. Contribution of TRPV1 to microglia-derived IL-6 and NFkappaB translocation with elevated hydrostatic pressure. *Invest Ophthalmol Vis Sci*. 2008;49:3004–3017.
98. Chidlow G, Wood JP, Ebneter A, Casson RJ. Interleukin-6 is an efficacious marker of axonal transport disruption during experimental glaucoma and stimulates neuritogenesis in cultured retinal ganglion cells. *Neurobiol Dis*. 2012;48:568–581.
99. Sims SM, Holmgren L, Cathcart HM, Sappington RM. Spatial regulation of interleukin-6 signaling in response to neurodegenerative stressors in the retina. *Am J Neurodegener Dis*. 2012;1:168–179.
100. Wilson GN, Inman DM, Dengler Crish CM, Smith MA, Crish SD. Early pro-inflammatory cytokine elevations in the DBA/2J mouse model of glaucoma. *J Neuroinflam*. 2015;12:176.
101. Sappington RM, Chan M, Calkins DJ. Interleukin-6 protects retinal ganglion cells from pressure-induced death. *Invest Ophthalmol Vis Sci*. 2006;47:2932–2942.
102. Mendonca Torres PM, de Araujo EG. Interleukin-6 increases the survival of retinal ganglion cells in vitro. *J Neuroimmunol*. 2001;117:43–50.
103. Leibinger M, Zeitler C, Gobrecht P, Andreadaki A, Gisselmann G, Fischer D. Transneuronal delivery of hyper-interleukin-6 enables functional recovery after severe spinal cord injury in mice. *Nat Commun*. 2021;12:391.
104. Leibinger M, Muller A, Gobrecht P, Diekmann H, Andreadaki A, Fischer D. Interleukin-6 contributes to CNS axon regeneration upon inflammatory stimulation. *Cell Death Dis*. 2013;4:e609.
105. Fisher J, Mizrahi T, Schori H, et al. Increased post-traumatic survival of neurons in IL-6-knockout mice on a background of EAE susceptibility. *J Neuroimmunol*. 2001;119:1–9.
106. Echevarria FD, Formichella CR, Sappington RM. Interleukin-6 Deficiency Attenuates Retinal Ganglion Cell Axonopathy and Glaucoma-Related Vision Loss. *Front Neurosci*. 2017;11:318.

Investigative Ophthalmology & Visual Science